Role of oblique convergence in the active deformation of the Himalayas and southern Tibet plateau

Robert McCaffrey
Department of Earth and Environmental Sciences, Rensselaer Polytechnic Institute, Troy, New York 12180
John Nabelek
College of Oceanic and Atmospheric Sciences, Oregon State University, Corvallis, Oregon 97331

ABSTRACT

Noting similarities with subduction along curved oceanic trenches and using a simple block model, we show that radial vergence evident in earthquake slip vectors along the Himalayan deformation front, east-west extension on north-trending normal faults in the Himalayas and southern Tibet, and right-lateral strike slip on the Karakorum-Jiali fault zone can all result from basal shear caused by the Indian plate sliding obliquely beneath Tibet along a gently dipping, arcuate plate boundary. Within the framework of this mechanism, the normal faults in the Himalayas and southern Tibet are not proxies for the uplift history of Tibet. The distribution and style of the faults in the Himalayas and southern Tibet suggest that the basal drag from the underthrusting Indian lithosphere extends northward beneath most of southern Tibet.

INTRODUCTION

Forearcs of many subduction zones undergo rapid arc-parallel extension, revealed by a systematic rotation of interplate earthquake slip vectors away from expected plate convergence directions (McCaffrey, 1996). In extreme cases, such as the Marianas, New Hebrides, and Sumatra, slip vectors are nearly radial (perpendicular to the trench) despite large lateral changes in convergence obliquity between the major plates. Pure thrusting during plate boundary earthquakes indicates that the trench-parallel force in the upper plate arising from oblique convergence is not balanced elastically but instead produces permanent deformation. For example, oblique convergence in Sumatra results in a trench-parallel strike-slip fault 300 km from the trench and trench-parallel extension of the forearc above the dipping plate boundary (McCaffrey et al., 1997). In the Aleutians, trench-parallel motion is taken up by large, submarine forearc blocks over the plate interface that translate, separate, and rotate (Geist et al., 1988). Such upper plate shear and extension is caused by subduction beneath a curved margin (Avé Lallemant and Guth, 1990; McCaffrey, 1992).

The active tectonics of the Himalayas and the southern half of Tibet where they interact with the underthrusting Indian plate (Fig. 1) show a strong resemblance to subduction at curved oceanic trenches. Slip vectors of thrust earthquakes at the curved Himalayan deformation front are normal to it. Seismicity (Molnar and Lyon-Caen, 1989) and active north-south–trending grabens (Armijo et al., 1986) show that the Himalayas and southern Tibet are extending in the east-west direction. A right-lateral, strike-slip shear zone across southern Tibet is roughly parallel to the deformation front (Armijo et al., 1989). Similarities between the surface deformation in Tibet and in upper plates at subduction zones suggest that the deformation in both settings is caused by a common mechanism (McCaffrey, 1992). As we show with a block model, basal shear arising from relative motion beneath an arcuate upper plate can reproduce the observed deformation in southern Tibet. We thus infer that some part of the Indian lithosphere thrusts beneath most of the southern half of Tibet, resulting in east-west extension in the Himalayas and southern Tibet (McCaffrey et al., 1996).

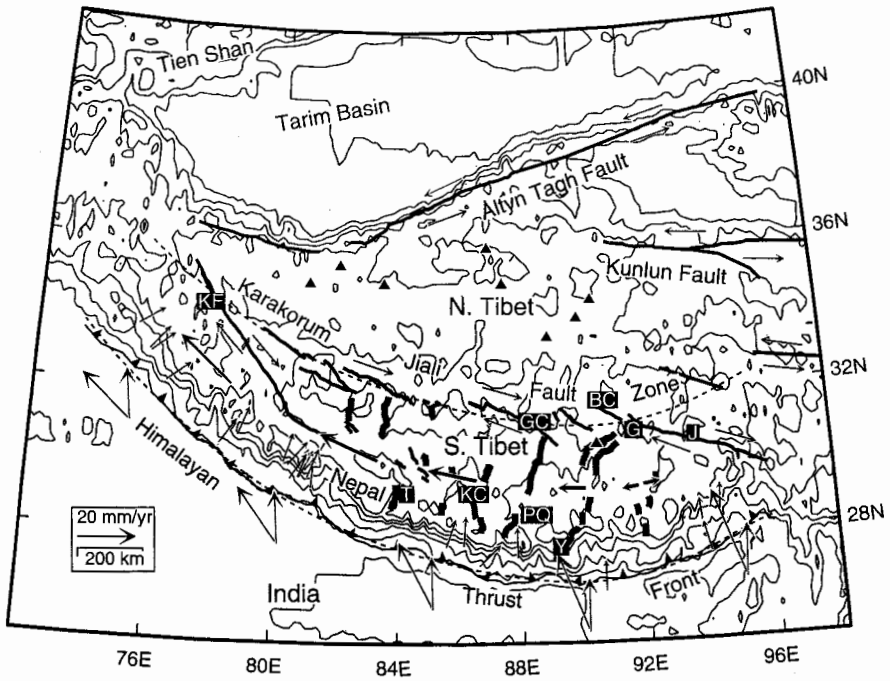

Figure 1. Major faults associated with oblique convergence between India and Tibet. Thrust faults are shown by black lines with barbs, strike-slip faults by heavy black lines with opposing arrows, and extensional grabens by thicker gray lines. Slip vectors of thrust earthquakes (small, thin vectors) show direction of India moving beneath Himalayas. Large black vectors south of thrust front show convergence of India with northern Tibet using a pole that includes slip on Altyn Tagh fault, and gray vectors are from NUVEL-1A India-Eurasia pole with angular velocity divided by three. Heavy arrows in southern Tibet show predicted velocities of southern Tibet relative to northern Tibet for full partitioning. Labeled normal faults are Thakkola (T), Kung Co (KC), Pum Qu (PQ), Yadong (Y), and Gulu (G). Strike-slip faults are Karakorum (KF), Gyaring Co (GC), Beng Co (BC), and Jiali (J). Dashed lines show smoothed outline of deformation front, used in partitioning calculations, and its projection onto Karakorum-Jiali fault zone. Topographic contour interval is 1 km, and triangles show Cenozoic volcanoes (Molnar et al., 1993).

BLOCK MODEL OF OBLIQUE CONVERGENCE

A simple block model illustrates how radial slip vectors, margin-parallel extension, and translation of the leading edge of the upper plate all result from subduction beneath a curved plate boundary. We use a rigid quarter circle backstop and align small wooden blocks along its curved edge (Fig. 2, A and B). We push the backstop over the base and digitize the paths of the blocks. The motions of the blocks relative to the base are analogous to earthquake slip-vectors (Fig. 2C) and motions relative to the backstop (Fig. 2D) reveal along-strike translation and extension of the forearc (Fig. 2, E and F).

Block motions are governed by a force balance as described more generally by McCaffrey (1992) for oblique subduction. The convergence obliquity γ is the angle between the local normal to the backstop n and the direction the backstop is moving. As the backstop moves, the shear force on the base of a forearc block has a component tangent to the backstop equal to $\sigma_b A_b \sin \gamma$, where σ_b is the basal shear stress and A_b is the basal area of the block. This basal force is balanced by the shear force of $\sigma_y A_v$ on the vertical boundary between the backstop and the block. If σ_y is the yield stress for slip along the backstop boundary and ψ is the smallest obliquity at which the block will slide relative to the backstop, then a force balance at obliquities of $\gamma \geq \psi$ gives

$$\sin \psi = \sigma_y A_v / \sigma_b A_b . \quad (1)$$

Because the shear stress on the backstop boundary cannot exceed σ_y, the direction the block moves over the base relative to n cannot exceed ψ. When ψ is small, slip-vectors are nearly parallel to n, that is, perpendicular to the deformation front. Knowing ψ, the velocity at which the forearc block moves along the backstop is

$$v_t = v (\sin \gamma - \cos \gamma \tan \psi) \quad (2)$$

when $\gamma \geq \psi$, and $v_t = 0$ when $\gamma < \psi$, where v is the velocity of the backstop relative to the surface beneath (Fig. 2E). Positive gradients in v_t, that is, arc-parallel stretching of a forearc, can result from along-strike variations in convergence rate, obliquity, or strengths of the thrust or upper plate faults. Specific examples include: (1) The backstop is straight and ψ decreases along strike due to an increase in basal shear or a decrease in vertical shear along the backstop; (2) the pole of rotation is located such that γ increases along strike; and (3) like most oceanic forearcs, the backstop is convex toward the subducting plate. We focus on the third case because the Himalayan front is convex toward India, but a nearby pole of rotation may also contribute to the along-strike variation in obliquity.

Margin-parallel stretching will occur at a rate of

$$dv_t/ds = r^{-1} dv_t/d\gamma = r^{-1} v (\cos \gamma + \sin \gamma \tan \psi) \quad (3)$$

when $\gamma \geq \psi$, and $dv_t/ds = 0$ when $\gamma < \psi$, where s is the distance along strike, r is the radius of the arc, and $ds = r\, d\gamma$. Equations 1 through 3 predict that as the backstop is pushed, we will see (1) blocks at the leading edge of the backstop (where $\gamma < \psi$) moving with the backstop; (2) at obliquity $\gamma \geq \psi$, blocks moving slowly relative to the backstop but separating rapidly; (3) at highest obliquities $\gamma >> \psi$, blocks moving fastest relative to the backstop but having slow separation rates; and (4) the blocks' motion over the base forms an angle ψ with the normal to the backstop. Our block experiment (Fig. 2) reveals these features in quantitative agreement with theory. In particular, because ψ is small, the blocks have nearly radial slip vectors (Fig. 2C).

For similar partitioning to occur in the Earth, the underlying plate interface must be able to generate a stress large enough to cause normal and strike-slip faults in the overriding plate to fail. The force needed to stretch the forearc adds to the numerator of the right side of equation 1, but if the numerator remains less than 1, then partitioning will still occur according to equations 2 and 3.

APPLICATION TO INDIA-TIBET CONVERGENCE

Figure 1 reveals patterns of deformation and slip vectors in the Himalayas and southern Tibet similar to the block model (Fig. 2). In this analogy, India forms the base of the model, northern Tibet (north of the Karakorum-Jiali fault zone) is the backstop, and the Himalayas and southern Tibet, between the deformation front and the

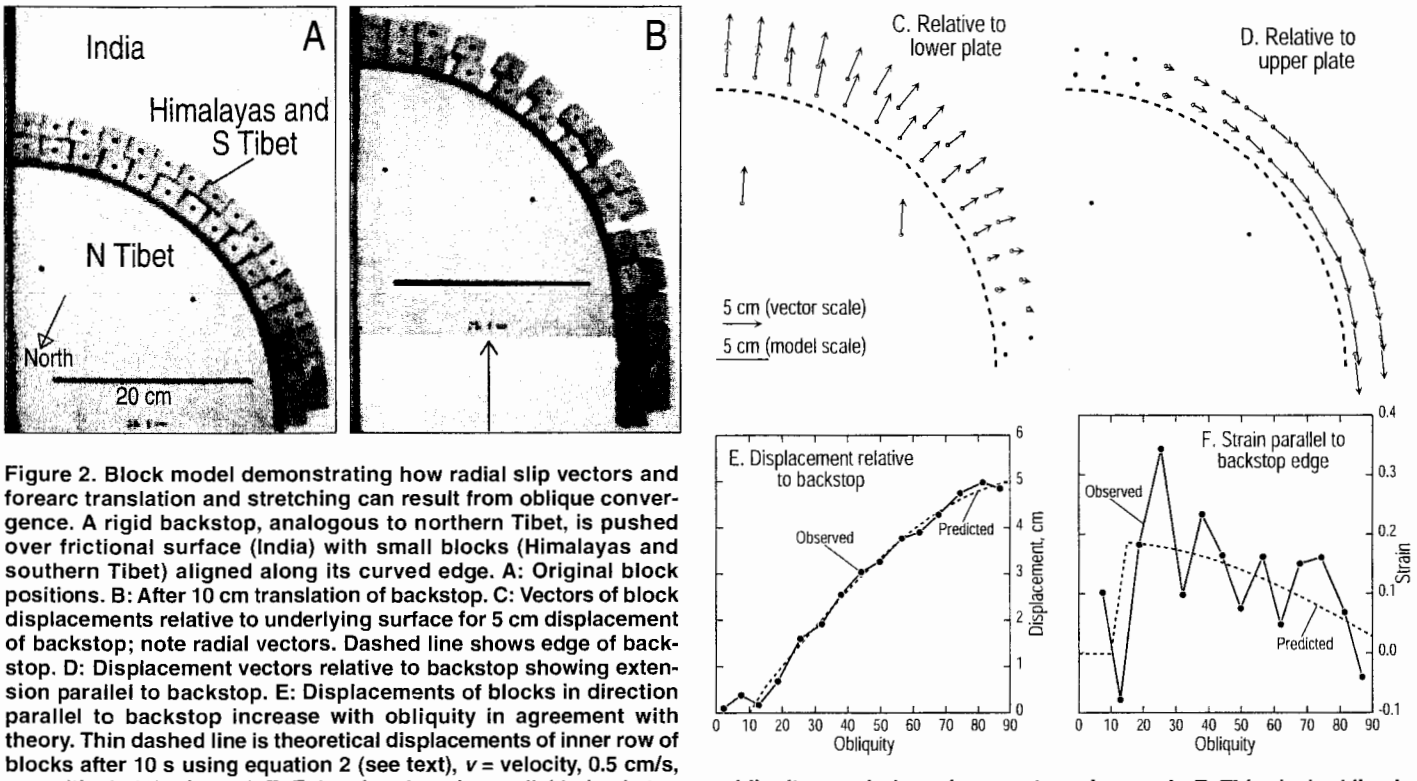

Figure 2. Block model demonstrating how radial slip vectors and forearc translation and stretching can result from oblique convergence. A rigid backstop, analogous to northern Tibet, is pushed over frictional surface (India) with small blocks (Himalayas and southern Tibet) aligned along its curved edge. A: Original block positions. B: After 10 cm translation of backstop. C: Vectors of block displacements relative to underlying surface for 5 cm displacement of backstop; note radial vectors. Dashed line shows edge of backstop. D: Displacement vectors relative to backstop showing extension parallel to backstop. E: Displacements of blocks in direction parallel to backstop increase with obliquity in agreement with theory. Thin dashed line is theoretical displacements of inner row of blocks after 10 s using equation 2 (see text), v = velocity, 0.5 cm/s, ψ = critical obliquity, 10°. F: Extensional strain parallel to backstop vs. obliquity; symbols and parameter values as in E. Thin dashed line is predicted strain using equation 3 (see text); r = arc radius, 27 cm. Scatter is caused by small uncertainties in digitizing block positions, by block rotations, and by nonuniform strain in block model.

Karakorum-Jiali fault zone, is the region we call the forearc blocks. Within the Himalayas and southern Tibet, from 82°E to 92°E, extension is revealed by normal faults and earthquakes. West of 82°E, extension appears to be minor, yet translation is relatively rapid (along the Karakorum fault). As in the block model, slip vectors are perpendicular to the deformation front all along the Himalayas. Hence, oblique thrusting of India beneath the Himalayas and southern Tibet can account for first-order tectonic features of the southern margin of the India-Tibet collision.

The average rates of shearing across vertical planes parallel to the deformation front and east-west extension in the Himalayas and southern Tibet can be estimated quantitatively from equations 2 and 3 by knowing the pole of rotation between India and northern Tibet, the orientation of the Himalayan thrust fault, and the angle ψ (Fig. 3). Slip vectors at the Himalayan front show that $\psi \approx 0$. We assume that the strike slip faults west of 88°E, which are largely parallel to the deformation front, take up all the shear. Because the slip rate on an individual fault depends on its orientation relative to the expected margin-parallel shear, we separately estimate slip rates for the Jiali strike-slip faults east of 88°E that are oblique to the maximum shear direction (Fig. 1).

The calculated motion between India and northern Tibet depends on the assumed slip rate along the Altyn Tagh fault. If there is no slip on the Altyn Tagh fault, a reasonable estimate of the pole between India (I) and northern Tibet (NT) is the modern India-Eurasia pole (DeMets et al., 1994), but with angular velocity reduced by a factor of three (called the I-NT_N pole) to allow for convergence taken up within Asia. This pole predicts northward convergence all along the margin (Fig. 1), resulting in shearing rates that are much smaller than observed slip rates on the Karakorum-Jiali fault zone (Fig. 3). It predicts a fairly uniform along-strike margin-parallel extensional strain rate in Himalayas and southern Tibet with a factor of two increase in southeastern Tibet (Fig. 3), where the largest normal faults are found.

A better match to the deformation can be obtained with a pole that includes slip on the Altyn Tagh fault (Fig. 3). From a plate circuit of India, northern Tibet, the Tarim basin, and Eurasia, and assuming a slip rate of 25 ± 5 mm/yr on the Altyn Tagh fault (Peltzer et al., 1989) and a shortening rate of 17 ± 3 mm/yr across the Tien Shan (Abdrakhmatov et al., 1996), the pole of rotation between India and northern Tibet (I-NT_{ATF}; 12°N, 57°E, angular velocity 0.46° ± 0.07° per m.y.) predicts convergence perpendicular to the deformation front at 94°E and higher obliquity to the northwest (Fig. 1). The I-NT_{ATF} pole also predicts a maximum in the margin-parallel extensional strain rate in the southeast Himalayas and southern Tibet, but unlike the I-NT_N pole, it predicts a westward decrease in strain rate to near zero in the northwest Himalayas (Fig. 3). Therefore, the I-NT_{ATF} pole predicts the block southwest of the Karakorum fault to be fairly rigid but translating at about 20 mm/yr northwest relative to northern Tibet, and, as observed, extension to be concentrated in the southeast Himalayas and southeast Tibet.

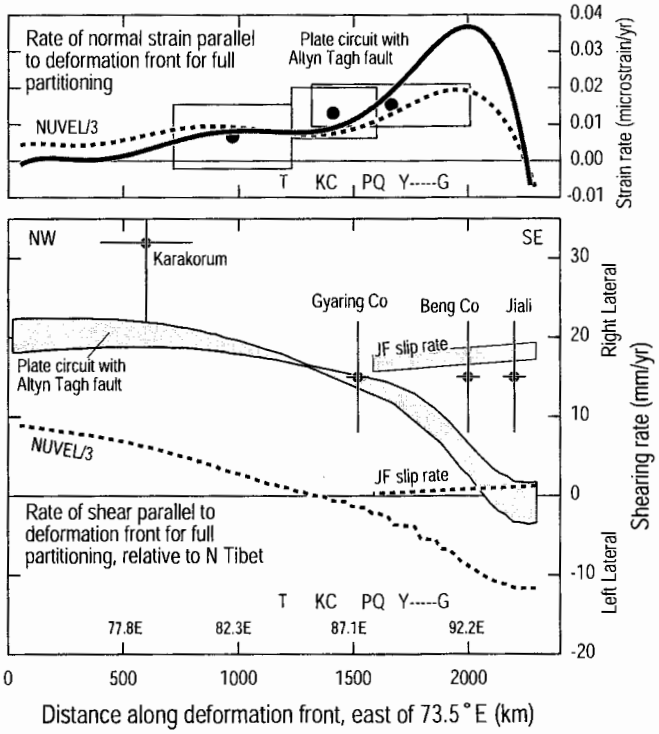

Figure 3. Predictions of shearing and margin-parallel extensional strain rates across Himalayas and southern Tibet based on partitioning of oblique convergence. Distance axis is along deformation front, labeled with approximate longitudes. In bottom panel, stippled curve shows rate of motion of outer edge of upper plate relative to northern Tibet in direction parallel to Himalayan deformation front based on equation 2 (see text), $\psi = 0$, and pole between India and northern Tibet that includes slip on Altyn Tagh fault. Curve labeled NUVEL/3 is calculated the same way, but uses India-Eurasia pole from NUVEL-1A with angular velocity divided by three. Lines labeled JF slip rate show expected slip rates (for both rotation poles) on Jiali fault, which differ from shearing rate due to Jiali fault not being parallel to deformation front. Dots with error bars show geologic slip rates on Karakorum (Searle, 1996) and on eastern strike-slip faults (Armijo et al., 1989). Top panel shows predicted margin-parallel extensional strain rates for two poles of rotation. Boxes show margin-parallel strain rates estimated from Global Positioning System measurements (Larson et al., 1997); height of box is ±1 standard deviation and width of box shows along-strike extent of regions used to calculate strain rate. Strain rates are consistent with either pole and show predicted eastward increase in strain rate. T, KC, PQ, and Y–G (see Fig. 1) show projections of large normal faults.

DISCUSSION

Several models have been proposed for the tectonics of Tibet but few have successfully predicted east-west extension in the Himalayas and southern Tibet. None have considered the basal shear that India applies to the Himalayas and southern Tibet. In a popular view, extension in the Himalayas and southern Tibet is thought to be due to gravitational collapse of the Tibetan plateau following uplift that resulted from sinking of the thickened mantle beneath Tibet either catastrophically (England and Houseman, 1989) or gradually (Lenardic and Kaula, 1995). It has been suggested that this plateau uplift also produced a change in monsoon activity in Asia and folding in the Indian Ocean lithosphere, as summarized by Molnar et al. (1993). According to England and Houseman (1989), the onset of normal faulting coincides with rapid uplift of the plateau; if true, this provides a means of dating the uplift history with the normal faults. In contrast, the occurrence of similar faulting in the submarine Aleutian forearc (Geist et al., 1988) shows that neither high elevation nor a rapid change in elevation are required for upper plate margin-parallel extension to occur. In our proposed mechanism, extension is driven by basal shear and can occur in the upper plate at any elevation.

Published constraints on the onset of extension in Himalayas and Southern Tibet support our claim. Harrison et al. (1995) demonstrated that the largest rift, the Yadong-Gulu (Fig. 1), initiated between 11 and 8 Ma and was extending rapidly at 8 Ma, in which case an intensification of extension may coincide with climate change and Indian Ocean deformation. Mercier et al. (1987) observed that east-west extension began in the Thakkhola graben in the Himalayas (Fig. 1) between 11 and 5 Ma. Coleman and Hodges (1995) argued for extension starting earlier than 14 Ma although the relevance of this age to east-west extension is not widely accepted (Harrison et al., 1995). Yin et al. (1994) observed a sparse, north-trending dike set, indicators of east-west extension, near the Tsangpo suture beginning 15 to 18 Ma. Harrison et al. (1995) explained the geographic distribution of ages by invoking different extension mechanisms to be active in Tibet's

geological history. In our mechanism, margin-parallel extension can extend all the way to the deformation front, as recent Global Positioning System measurements confirm (Larson et al., 1997). Hence, we argue that normal faults in both southern Tibet and the Himalayas have the same underlying cause. To the degree that the dikes reported by Yin et al. (1994) indicate east-west extension, this mechanism was already operating by 15 to 18 Ma. Extension could be even older than 18 Ma because, like most subduction zones, the original deformation front was probably curved from the beginning of the collision. However, if extension in southern Tibet did accelerate at about 10 Ma or earlier, then a possible explanation is that the Altyn Tagh fault was initiated about that time.

Whereas explanations that restrict extension to high elevations predict that normal faulting should be at least as prevalent in northern Tibet as it is in southern Tibet, the grabens in southern Tibet appear to be largely truncated in the north by the Jiali fault zone (Armijo et al., 1986, 1989). Our mechanism localizes the normal faulting in the Himalayas and southern Tibet above areas having basal shear from the under-thrusting Indian lithosphere. On the basis of experiments with multiple rows of blocks, observations from subduction zones, and reasoning that upper plate shear strain concentrates near boundaries where basal tractions are varying, we suggest that the Karakorum-Jiali fault zone marks the northern termination of the strong basal shear beneath southern Tibet.

Our model does not require wholesale subduction of Indian lithosphere with crust intact. It is more likely that the Indian crust is detached from its mantle and is incorporated into the thickened crust of Tibet (Nelson et al., 1996). In our view, some part of India's mantle continues to slide below southern Tibet along a gently dipping plane. All of southern Tibet is underlain by high-seismic-velocity mantle, which is likely that of India, whereas the northern Tibet mantle has low seismic velocity (Owens and Zandt, 1997). Small earthquakes as deep as 90 km are found only beneath southern Tibet, indicating an upper mantle that is relatively cold and capable of maintaining shear stress (Chen and Kao, 1996).

The largest uncertainty in our partitioning model arises from the unknown pole of rotation between India and northern Tibet, which determines the slip rates to be expected on the Karakorum-Jiali fault zone. We favor a high slip rate on the Altyn Tagh fault, not only because it matches the distribution of normal faulting in the Himalayas and southern Tibet and slip rates on the Karakorum-Jiali fault zone, but also because late initiation of the Altyn Tagh fault offers a possible mechanism for triggering normal and strike-slip faulting late in the history of the collision.

We have shown that the common process of partitioning oblique convergence in response to drag from the downgoing plate simultaneously produces radial slip vectors, along-strike translation, and extension parallel to the deformation front, all observed features of the Himalayas and southern Tibet. In addition to the agreement between our model and the limited data available for Tibet, support for our hypothesis comes also from its relevance to convergent margin tectonics in many other parts of the world.

ACKNOWLEDGMENTS

We thank P. Molnar for discussions, K. Larson and R. Bilham for sharing unpublished geodetic results from Nepal, and W.-P. Chen, W. S. F. Kidd, and L. Ratschbacher for helpful reviews.

REFERENCES CITED

Abdrakhmatov, K. Y., Aldazhanov, S. A., Hager, B. H., Hamburger, M. W., Herring, T. A., Kalabaev, K. B., Makarov, V. I., Molnar, P., Panasyuk, S. V., Prilepin, M. T., Reilinger, R. E., Sadybakasov, I. S., Souter, B. S., Trapeznikov, Y. A., Tsurkov, V. Y., and Zubovich, A. V., 1996, Relatively recent construction of the Tien Shan inferred from GPS measurements of present-day crustal deformation rates: Nature, v. 384, p. 450–453.

Armijo, R., Tapponnier, P., Mercier, J. L., and Han, T. L., 1986, Quaternary extension in southern Tibet: Field observations and tectonic implications: Journal of Geophysical Research, v. 91, p. 13803–13872.

Armijo, R., Tapponnier, P., and Tonglin, H., 1989, Late Cenozoic right-lateral strike-slip faulting in southern Tibet: Journal of Geophysical Research, v. 94, p. 2787–2838.

Avé Lallemant, H. G., and Guth, L. R., 1990, Role of extensional tectonics in exhumation of eclogites and blueschists in an oblique subduction setting, northwest Venezuela: Geology, v. 18, p. 950–953.

Chen, W.-P., and Kao, H., 1996, Seismotectonics of Asia: Some recent progress, *in* Yin, A., and Harrison, M., eds., The tectonic evolution of Asia: Palo Alto, California, Cambridge University Press, p. 37–62.

Coleman, M., and Hodges, K., 1995, Evidence for Tibetan plateau uplift before 14 Myr ago from a new minimum age for east-west extension: Nature, v. 374, p. 49–52.

DeMets, C., Gordon, R. G., Argus, D. F., and Stein, S., 1994, Effects of recent revisions to the geomagnetic reversal time scale on estimates of current plate motions: Geophysical Research Letters, v. 21, p. 2191–2194.

England, P., and Houseman, G., 1989, Extension during continental convergence, with application to the Tibetan Plateau: Journal of Geophysical Research, v. 94, p. 17561–17579.

Geist, E. L., Childs, J. R., and Scholl, D. W., 1988, The origin of summit basins of the Aleutian Ridge: Implications for block rotation of an arc massif: Tectonics, v. 7, p. 327–341.

Harrison, T. M., Copeland, P., Kidd, W. S. F., and Lovera, O. M., 1995, Activation of the Nyainqentanghla shear zone: Implications for uplift of the southern Tibetan Plateau: Tectonics, v. 14, p. 658–676.

Larson, K., Burgmann, R., and Bilham, R., 1997, Kinematics of the India-Eurasia collision zone [abs.]: Eos (Transactions, American Geophysical Union), v. 78, p. F168.

Lenardic, A., and Kaula, W. M., 1995, More thoughts on convergent crustal plateau formation and mantle dynamics with regard to Tibet: Journal of Geophysical Research, v. 100, p. 15193–15203.

McCaffrey, R., 1992, Oblique plate convergence, slip vectors, and forearc deformation: Journal of Geophysical Research, v. 97, p. 8905–8915.

McCaffrey, R., 1996, Estimates of modern arc-parallel strain rates in fore arcs: Geology, v. 24, p. 27–30.

McCaffrey, R., Nabelek, J., and Zwick, P., 1996, Role of oblique convergence in the active deformation of southern Tibet [abs.]: Eos (Transactions, American Geophysical Union), v. 77, p. F693.

McCaffrey, R., Zwick, P., Bock, Y., Genrich, J., Subarya, C., and Puntodewo, S. S. O., 1997, Geodetic evidence for full strain partitioning in north Sumatra [abs.]: Eos (Transactions, American Geophysical Union), v. 78, p. F168.

Mercier, J.-L., Armijo, R., Tapponnier, P., Carey-Gailhardis, E., and Han, T. L., 1987, Change from Tertiary compression to Quaternary extension in southern Tibet during the India-Eurasia collision: Tectonics, v. 6, p. 275–304.

Molnar, P., and Lyon-Caen, H., 1989, Fault plane solutions of earthquakes and active tectonics of the Tibetan Plateau and its margins: Geophysical Journal International, v. 99, p. 123–153.

Molnar, P., England, P., and Martinod, J., 1993, Mantle dynamics, uplift of the Tibetan Plateau, and the Indian monsoon: Review of Geophysics, v. 31, p. 357–396.

Nelson, K. D., Zhao, W., Brown, L., Kuo, J., Che, J., Liu, X., Klemperer, S., Makovsky, Y., Meissner, R., Mechie, J., Kind, R., Wenzel, F., Ni, J., Nabelek, J., Leshou, C., Tan, H., Wei, W., Jones, A., Booker, J., Unsworth, M., Kidd, W., Hauck, M., Alsdorf, D., Ross, A., Cogan, M., Wu, C., Sandvol, E., and Edwards, M., 1996, Partially molten middle crust beneath Southern Tibet: Synthesis of project INDEPTH results: Science, v. 274, p. 1684–1688.

Owens, T. J., and Zandt, G., 1997, Implications of crustal property variations for models of Tibetan plateau evolution: Nature, v. 387, p. 37–43.

Peltzer, G., Tapponnier, P., and Armijo, R., 1989, Magnitude of late Quaternary left-lateral displacements along the north edge of Tibet: Science, v. 246, p. 1285–1289.

Searle, M. P., 1996, Geological evidence against large-scale pre-Holocene offsets along the Karakorum fault: Implications for the limited extrusion of the Tibetan Plateau: Tectonics, v. 15, p. 171–186.

Yin, A., Harrison, T. M., Ryerson, F. J., Chen, W., Kidd, W. S. F., and Copeland, P., 1994, Tertiary structural evolution of the Gangdese thrust system, southeastern Tibet: Journal of Geophysical Research, v. 99, p. 18175–18201.

Manuscript received January 28, 1998
Revised manuscript received April 30, 1998
Manuscript accepted May 11, 1998